Identification of FIP200 interaction with the TSC1–TSC2 complex and its role in regulation of cell size control

Boyi Gan,[1] Zara K. Melkoumian,[1] Xiaoyang Wu,[1] Kun-Liang Guan,[2] and Jun-Lin Guan[1]

[1]Department of Molecular Medicine, College of Veterinary Medicine, Cornell University, Ithaca, NY 14853
[2]Life Sciences Institute, University of Michigan, Ann Arbor, MI 48109

FIP200 (focal adhesion kinase [FAK] family interacting protein of 200 kD) is a newly identified protein that binds to the kinase domain of FAK and inhibits its kinase activity and associated cellular functions. Here, we identify an interaction between FIP200 and the TSC1–TSC2 complex through FIP200 binding to TSC1. We found that association of FIP200 with the TSC1–TSC2 complex correlated with its ability to increase cell size and up-regulate S6 kinase phosphorylation but was not involved in the regulation of cell cycle progression. Conversely, knockdown of endogenous FIP200 by RNA interference reduced S6 kinase phosphorylation and cell size, which required TSC1 but was independent of FAK. Furthermore, overexpression of FIP200 reduced TSC1–TSC2 complex formation, although knockdown of endogenous FIP200 by RNA interference did not affect TSC1–TSC2 complex formation. Lastly, we showed that FIP200 is important in nutrient stimulation-induced, but not energy- or serum-induced, S6 kinase activation. Together, these results suggest a cellular function of FIP200 in the regulation of cell size by interaction with the TSC1–TSC2 complex.

Introduction

FIP200 (FAK family interacting protein of 200 kD) is a newly identified protein inhibitor for FAK and its related kinase Pyk2 (Ueda et al., 2000; Abbi et al., 2002). It is a 1,591-aa protein with a large coiled-coil region (residues 860–1391) containing a leucine zipper motif (residues 1371–1391). FIP200 is a conserved protein present in human, mouse, rat, *Xenopus laevis,* and *Drosophila melanogaster*. Like FAK, FIP200 is widely expressed in various human tissues. FIP200 gene localizes in 8q11 chromosome (Chano et al., 2002b), containing several loci of putative tumor suppressor genes, and loss of heterozygosity for this region has been associated with breast cancer (Dahiya et al., 1998). We recently showed that association of endogenous FIP200 with FAK correlated with FAK inactivation upon cell detachment. Overexpression of FIP200 inhibited FAK kinase activity and autophosphorylation as well as its associated cellular functions including cell spreading, cell migration, and cell cycle progression. Conversely, disruption of the functional interaction between endogenous FIP200 with FAK led to increased FAK phosphorylation and partial restoration of cell cycle progression in cells plated on poly-L-lysine. These results identify FIP200 as a novel protein inhibitor for FAK (Abbi et al., 2002).

FIP200 is also identified by Chano et al. (2002a) independently as a potential regulator of the RB1 gene (designated by this group as RB1CC1 for RB1-inducible coiled-coil 1, but will be referred to here as FIP200 for convenience). The expression levels of FIP200 correlated with those of RB1 in various cancer cell lines and normal human tissues. In addition, FIP200 and RB1 are preferentially coexpressed and contributed to the maturation of human embryonic musculoskeletal cells and may regulate the proliferative activity and maturation of tumor cells derived from these tissues (Chano et al., 2002d). Lastly, it was found that 20% of primary breast cancers that were screened contained large deletion mutations in FIP200 that are predicted to generate markedly truncated proteins (Chano et al., 2002c). These studies are consistent with our findings showing negative regulation of cell cycle progression by FIP200 (Abbi et al., 2002).

TSC1 and *TSC2* (or hamartin and tuberin, respectively) are both tumor suppressor genes and mutation in either gene causes tuberous sclerosis (TSC) that occurs in ~1 in 6,000 of the population and is defined by the formation of hamartomas in a wide range of tissues. Both TSC1 and TSC2 have coiled-coil regions and they exist as heterodimers (Plank et al., 1998;

Correspondence to J.-L. Guan: jg19@cornell.edu

Abbreviations used in this paper: FSC-H, forward scatter; MEF, mouse embryonic fibroblast; RNAi, RNA interference; S6K, S6 kinase; TSC, tuberous sclerosis.

The Journal of Cell Biology, Vol. 170, No. 3, August 1, 2005 379–389
http://www.jcb.org/cgi/doi/10.1083/jcb.200411106

van Slegtenhorst et al., 1998; Kwiatkowski, 2003). Although TSC1 has no known enzymatic activity, TSC2 contains a COOH-terminal GAP domain for the small G protein Rheb (Garami et al., 2003; Inoki et al., 2003a; Saucedo et al., 2003; Stocker et al., 2003; Tee et al., 2003; Y. Zhang et al., 2003). Recent studies have indicated that the TSC1–TSC2 complex regulates cellular functions mainly by their inhibition of mTOR and its targets S6 kinase (S6K) and 4E-BP1 (Potter et al., 2001; Tapon et al., 2001; Gao et al., 2002; Goncharova et al., 2002; Inoki et al., 2002; Manning et al., 2002; Tee et al., 2003). Increased S6K activity is observed in TSC mutations in *D. melanogaster*, cells derived from TSC1 or TSC2 knockout mice, or cells treated with TSC1 or TSC2 small interfering RNA. Consistent with its function as a negative regulator of mTOR and its targets, the TSC complex has been found to regulate various cellular functions such as cell cycle progression, cell size control, cell survival, and apoptosis (Hengstschlager et al., 2001; Inoki et al., 2003b; Shamji et al., 2003).

To investigate the molecular mechanisms by which FIP200 regulates intracellular signaling pathways and cellular functions, we used yeast two-hybrid screening to identify other proteins that interact with FIP200. Here, we report identification of FIP200 interaction with the TSC1–TSC2 complex and show that this interaction leads to inhibition of TSC1–TSC2 complex function resulting in increased S6K activity and cell growth. These studies suggest a novel function for FIP200 in the regulation of cell size control in addition to its functioning as an inhibitor for FAK and regulator of RB1 expression.

Results

Identification of FIP200 interaction with TSC1

To understand the mechanisms and potential role of FIP200 in signal transduction and regulation of cellular functions, we used the yeast two-hybrid screen to identify cellular proteins that interact with FIP200. Because the full-length FIP200 and its COOH-terminal part (containing the large coiled-coil region) showed strong autoactivation in the yeast two-hybrid system (unpublished data), we used the NH_2-terminal half of FIP200 (residues 1–859, designated as N1-859 here) as the bait. Screening $\sim 1 \times 10^6$ clones of a human heart library yielded several clones that specifically interacted with N1-859. Partial sequencing of the clones indicated that two clones (#16 and #34) encode a fragment of TSC1 (residues 304–1165; Fig. 1 A) and one (clone #16) was further analyzed. The interaction was confirmed by cotransforming yeast cells with the recovered prey plasmid pB42AD-#16 and pLexA-N1-859, pLexA, or pLexA-Lamin C encoding the irrelevant protein Lamin C as controls. We found that clone #16 interacted specifically with N1-859, but not with control Lamin C or the empty vector, in the yeast.

We next examined potential interaction of FIP200 with TSC1 in 293T cells. The insert from pB42AD-#16 was excised and cloned into a mammalian expression vector with Myc tag. The resulting vector encoding Myc-tagged TSC1 304–1165 was cotransfected into 293T cells along with pKH3-FIP200 encoding the HA-tagged FIP200. Cell lysates were immunoprecipitated with anti-HA antibody and followed by Western blotting with anti-Myc antibody. Fig. 1 B shows that Myc-TSC1 304–1165 (i.e., clone #16) was coprecipitated with HA-FIP200, but not detected in the immunoprecipitates of control lysates from cells cotransfected with pKH3 empty vector. Additional experiments using Myc-tagged full-length TSC1 and several segments indicated that FIP200 could interact with TSC1, its 403–787-aa region, but not with TSC1 1–402 and 789–1165 aa regions. We also detect the interaction of the FIP200 N1-859 fragment with TSC1 403–787 aa and full-length TSC1 (not depicted). Lastly, we found that recombinant

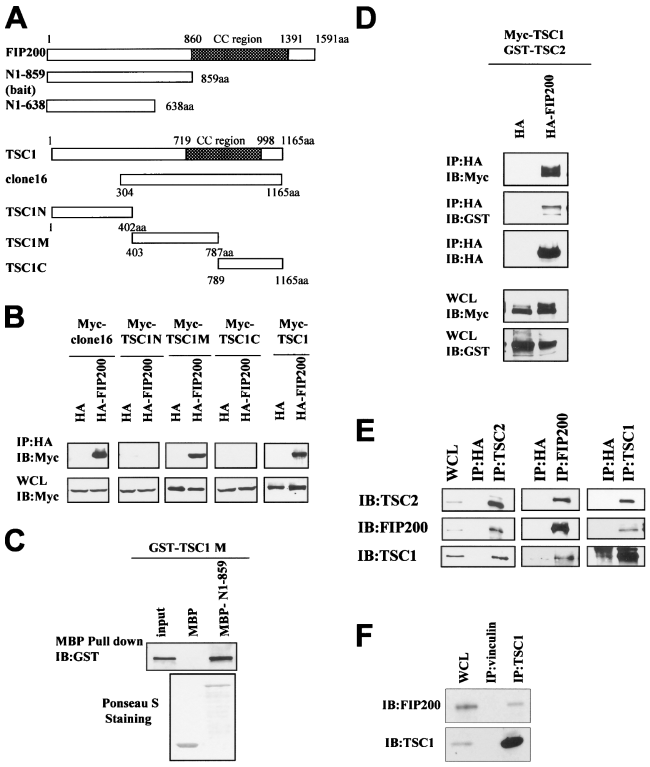

Figure 1. **Interaction of FIP200 with TSC1.** (A) Schematic diagram showing the region of FIP200 used as the bait for yeast two-hybrid screen and TSC1 prey and other segments used for binding studies. (B) 293T cells were cotransfected with vectors encoding the HA-FIP200 or vector control and plasmids encoding Myc-tagged TSC1 304–1165 aa (clone 16), other TSC1 segments, or full-length TSC1, as indicated. Cell lysates were immunoprecipitated with anti-HA and analyzed by Western blotting with anti-Myc to detect bound TSC1 segments. Aliquots of the lysates (WCL) were also analyzed directly by Western blotting with anti-Myc. (C) Purified GST-TSC1M was incubated with immobilized MBP fusion proteins containing the FIP200 N1-859 segment or MBP alone. The bound proteins along with an aliquot of input were resolved on SDS-PAGE and analyzed by Western blotting with anti-GST (top). The membrane was also stained with Ponceau S (bottom). (D) 293T cells were cotransfected with vectors encoding HA-FIP200 or vector control and plasmids encoding Myc-TSC1 and GST-TSC2. Aliquots of the lysates (WCL) or anti-HA immunoprecipitates from the lysates (IP: HA) were analyzed by Western blotting with anti-Myc, anti-GST, or anti-HA, as indicated. (E) Lysates prepared from 293T cells were immunoprecipitated by anti-FIP200, anti-TSC2, and anti-TSC1 to precipitate respective endogenous proteins or HA antibody as a control. They were then analyzed by Western blotting with anti-TSC2 (top), anti-FIP200 (middle), or anti-TSC1 (bottom) to detect the associated proteins. (F) Lysates from MEFs were immunoprecipitated by anti-TSC1 or anti-vinculin. They were then analyzed by Western blotting with anti-FIP200 (top) or anti-TSC1 (bottom). (E and F) Aliquots of the lysates (WCL) were also analyzed directly.

GST fusion protein containing TSC1 residues 403–787 bound to purified MBP fusion protein containing FIP200 N1-859, but not MBP alone, in vitro, suggesting a direct interaction between FIP200 and TSC1 (Fig. 1 C). Together, these results identify TSC1 as a FIP200 interacting protein and suggest that the interaction is mediated by the FIP200 1–859 aa region and the TSC1 403–787 aa region.

Association of FIP200 with the TSC1–TSC2 complex

TSC1 and TSC2 have been shown to function as a complex in vivo (Plank et al., 1998; van Slegtenhorst et al., 1998; Kwiatkowski, 2003). Therefore, we tested whether FIP200 could associate with the TSC1–TSC2 complex in cells. pKH3-FIP200 was cotransfected into 293T cells with plasmids encoding Myc-TSC1 and GST-TSC2. Lysates were prepared from the transfected cells and immunoprecipitated by anti-HA, and the associated proteins were analyzed by Western blotting by respective antibodies. Fig. 1 D shows that both TSC1 and TSC2 were coprecipitated with FIP200, but not in pKH3 control vector–transfected cells. Consistent with these transfection studies, we could also detect the interaction of endogenous FIP200 with the endogenous TSC1–TSC2 complex in 293T cells (Fig. 1 E). Both TSC1 and TSC2 were found in anti-FIP200 immunoprecipitates, but not in the control immunoprecipitates with an irrelevant antibody anti-HA. Likewise, FIP200 is also detected in both anti-TSC1 and -TSC2 immunoprecipitates, but not control immunoprecipitates. Lastly, coimmunoprecipitation of endogenous FIP200 with TSC1, but not vinculin, was also observed in mouse embryonic fibroblasts (MEFs; Fig. 1 F). Together, these results demonstrate that FIP200 could associate with the TSC1–TSC2 complex in mammalian cells such as 293T cells and MEFs.

FIP200 interaction with the TSC1-TSC2 complex is not involved in FIP200 regulation of cell cycle progression

Our previous studies showed that FIP200 plays an important role in the regulation of cell cycle progression (Abbi et al., 2002). Some studies also showed that the TSC1–TSC2 complex is capable of regulating cell proliferation (Soucek et al., 1998, 2001; Miloloza et al., 2000; Hengstschlager and Rosner, 2003). Thus, the identification of the interaction between FIP200 and the TSC1–TSC2 complex raises the possibility that this interaction may play a role in the regulation of cell cycle progression by FIP200. Indeed, the FIP200 N1-859 fragment, which can interact with the TSC1–TSC2 complex (Fig. 2 A), showed similar activity as the full-length FIP200 in the inhibition of cell cycle progression as measured by BrdU incorporation (not depicted). However, the smaller segment of FIP200 (N1-638; Fig. 1 A), which did not associate with the TSC1–TSC2 complex (Fig. 2 A), could also inhibit cell cycle progression (Abbi et al., 2002). These results suggest that FIP200 interaction with the TSC1–TSC2 complex might not be required for FIP200 regulation of cell cycle progression.

To further evaluate the role of the TSC1–TSC2 complex in cell cycle inhibition by FIP200, we examined the effects of

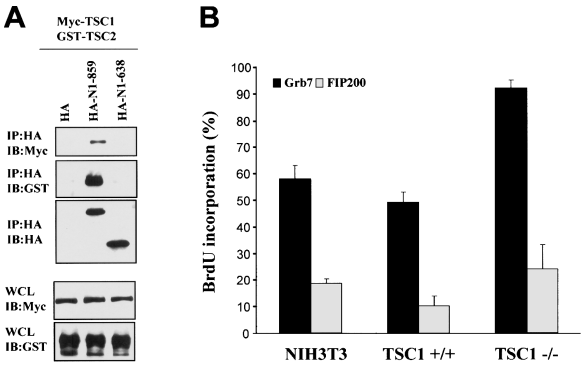

Figure 2. **FIP200 interaction with the TSC1–TSC2 complex is not required for FIP200 regulation of cell cycle progression.** (A) 293T cells were cotransfected with vectors encoding HA-N1-859 or HA-N1-638 or vector control and plasmids encoding Myc-TSC1 and GST-TSC2. Aliquots of the lysates (WCL) or anti-HA immunoprecipitates from the lysates (IP: HA) were analyzed by Western blotting with anti-Myc, anti-GST, or anti-HA, as indicated. (B) NIH 3T3, TSC1+/+, or TSC1−/− fibroblasts were transiently transfected with pKH3-FIP200 or pKH3-Grb7 control. They were then analyzed for BrdU incorporation as described previously (Zhao et al., 1998). The percentage of BrdU (+)/positively transfected cells (as identified by anti-HA staining) was determined by analyzing ~100 positively transfected cells for each transfection in multiple fields. The results show mean + SEM for at least three independent experiments.

FIP200 on cell cycle progression in TSC1-null fibroblasts derived from TSC1 knockout mice (Kwiatkowski et al., 2002). Cells were transiently transfected with pKH3-FIP200 or the control pKH3-Grb7 plasmid, and then serum-stimulated cell cycle progression was measured by BrdU incorporation assay as described previously (Zhao et al., 1998; Abbi et al., 2002). We observed that TSC1−/− MEFs exhibited increased rate of cell cycle progression compared with TSC1+/+ MEF or NIH 3T3 cells (Fig. 2 B). Nevertheless, FIP200 significantly inhibited BrdU incorporation in TSC1−/− MEFs as well as in TSC1+/+ MEF and NIH 3T3 cells, when compared with the control plasmid. Together, these data suggest that FIP200 interaction with the TSC1–TSC2 complex is not required for FIP200 regulation of cell cycle progression.

FIP200 function in cell size control

Recent studies have identified the TSC1–TSC2 complex as a key regulator of cell size control (Inoki et al., 2003b; Shamji et al., 2003). Therefore our identification of the interaction between FIP200 and the TSC1–TSC2 complex raises the interesting possibility that FIP200 may regulate cell size through interaction with the TSC1–TSC2 complex. To investigate this possibility directly, 293T cells were transiently transfected with an expression vector encoding FIP200 or an empty vector control and the effects on cell size were then measured by determining the mean forward scatter (mean FSC-H) with a flow cytometer. Fig. 3 A shows that overexpression of FIP200 in these cells led to a right-shift of the mean FSC-H distribution compared with the empty vector–transfected cells, which corresponds to an increase in the size of the FIP200-transfected populations of cells. Quantification of the data indicated an ~5% increase in the average cell size in the FIP200-transfected 293T cells (Fig. 3 B). This is likely to be an underestimation of

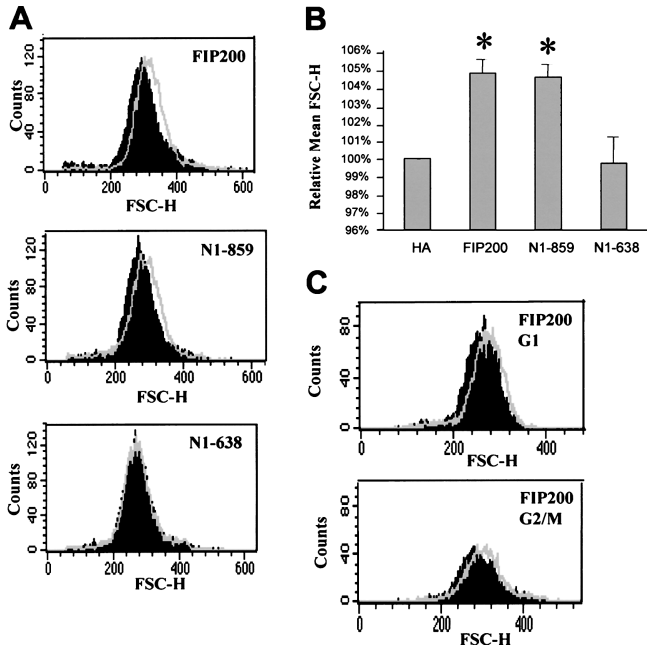

Figure 3. **FIP200 function in cell size control.** (A) 293T cells were transfected with vectors encoding HA-FIP200, HA-N1-859, HA-N1-638, or empty vector control. The cells were analyzed by FACS to determine cell size, as described in Materials and methods. Shown are histograms of mean FSC-H comparing cells transfected with FIP200 or its segments (gray lines) with cells transfected with the empty vector. Note that a right-shift of the mean FSC-H distribution reflects cell size increase. (B) Comparison of average size of cells transfected with FIP200 or its segments, as indicated. The results are normalized to cells transfected with empty vector and show relative mean FSC-H + SD for three independent experiments (*, $P < 0.001$ vs. control). (C) Histograms of mean FSC-H comparing cells transfected with FIP200 (gray lines) with cells transfected by the empty vector in G1 (top) and G2/M (bottom) phase population.

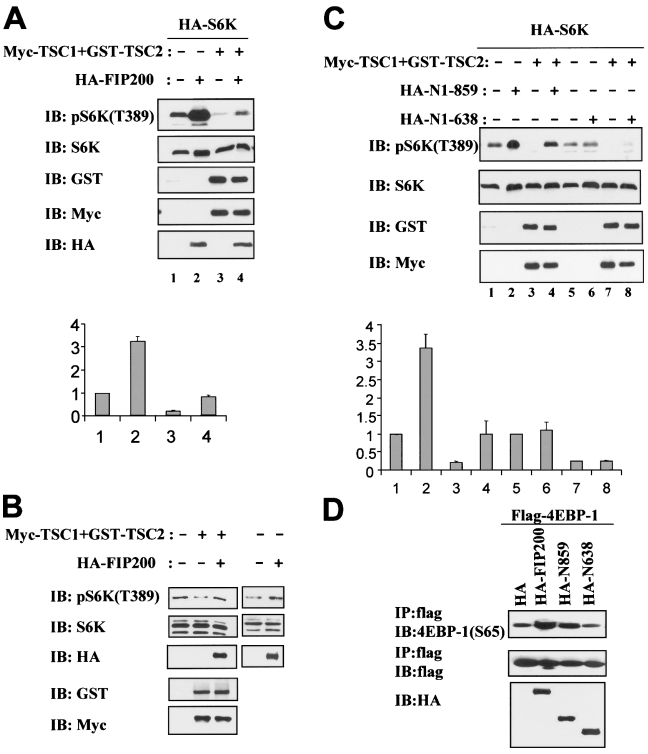

Figure 4. **Function of FIP200 association with TSC1–TSC2 in the regulation of S6K and 4EBP-1 phosphorylation.** (A–C) 293T cells were cotransfected with vectors encoding Myc-TSC1 and GST-TSC2 or empty vector control, HA-FIP200 (A and B), HA-N1-859 or HA-N1-638 (C), and HA-tagged S6K reporter plasmid (A and C), as indicated. 2 d after transfection, cell lysates were prepared and analyzed by Western blotting with anti-pS6K(T389) to detect activated HA-S6K reporter (A and C) or endogenous S6K (B) and other antibodies to verify expression levels of respective proteins, as indicated. Activated HA-S6K is normalized to the expression levels of HA-S6K in A and C and mean + SD for three independent experiments are shown on the bottom. (D) 293T cells were cotransfected with vectors encoding HA-FIP200, HA-N1-859, HA-N1-638, or empty vector control along with a Flag-tagged 4EBP-1 reporter plasmid. 2 d after transfection, cell lysates were immunoprecipitated by anti-Flag and analyzed by Western blotting with anti-p4EBP-1(S65) to detect activated Flag-4EBP-1 reporter (top) or anti-Flag to detect Flag-4EBP-1 expression levels (middle). Aliquots of lysates were also analyzed directly by Western blotting with anti-HA to verify expression levels of HA-FIP200 and its fragments (bottom).

the FIP200 effect on cell size as the transfection efficiency is <100% for these cells. Similar studies indicated that the N1-859 segment of FIP200, but not the N1-638 segment, which does not bind to TSC1–TSC2, also increased the average cell size of the transfected 293T cells (Fig. 3, A and B). Furthermore, the increase in cell size was observed in 293T cells in either G1 or G2/M phase (Fig. 3 C). Together, these results suggested a novel function for FIP200 in the regulation of cell size, possibly through its interaction with the TSC1–TSC2 complex.

FIP200 regulation of S6K phosphorylation through its association with the TSC1-TSC2 complex

Recent studies have shown that the TSC1–TSC2 complex negatively regulates cell size through inhibition of the mTOR–S6K pathway (Garami et al., 2003; Inoki et al., 2003a; Saucedo et al., 2003; Stocker et al., 2003; Tee et al., 2003; Y. Zhang et al., 2003). Therefore, we examined the possible effect of FIP200 on TSC1–TSC2 complex–mediated inhibition of S6K to determine the mechanisms by which FIP200 interaction with the TSC1–TSC2 complex regulated cell size. 293T cells were cotransfected with pKH3-FIP200 encoding HA-FIP200 or pKH3 empty vector along with plasmids encoding Myc-TSC1, GST-TSC2, and HA-tagged S6K. Cell lysates were then prepared and analyzed by Western blotting with anti-Thr389 phosphorylated S6K to determine its activation state or anti-S6K to verify similar expression levels of the protein in all samples. Consistent with previous observations (Inoki et al., 2002, 2003b), overexpression of TSC1 and TSC2 decreased S6K phosphorylation at Thr389 (Fig. 4 A, compare lanes 1 and 3). Interestingly, coexpression of FIP200 reversed the inhibition of S6K phosphorylation by the TSC1–TSC2 complex (Fig. 4 A, compare lane 4 with lanes 1 and 3). We also observed that overexpression of FIP200 alone increased S6K phosphorylation, possibly through its interaction with the endogenous TSC1–TSC2 complex (Fig. 4 A, compare lanes 1 and 2). Similarly, expression of FIP200 reversed inhibition of endogenous S6K phosphorylation by overexpression of the TSC1–TSC2 complex (Fig. 4 B, left) and expression of FIP200 alone also increased endogenous S6K phosphorylation (Fig. 4 B, right). It should be noted that the effects of FIP200 (and TSC also) on

endogenous S6K phosphorylation appears to be less pronounced than that using the transfected HA-S6K as a reporter. This is probably due to the <100% transfection efficiency in these cells. Furthermore, we found that overexpression of FIP200 N1-859, but not N1-638, fragment also increased S6K phosphorylation and reversed inhibition of S6K phosphorylation by the TSC1–TSC2 complex when coexpressed with TSC1 and TSC2 (Fig. 4 C). Consistent with the results on S6K phosphorylation, we also found that FIP200 and its fragment N1-859, but not N1-638 fragment, induced phosphorylation of 4E-BP1, another target of mTOR, in 293T cells (Fig. 4 D). Together, these results suggest that FIP200, through its N1-859 region association with the TSC1–TSC2 complex, may negatively regulate TSC1–TSC2 complex inhibition of the mTOR–S6K pathway, resulting in an increase in cell size.

We used RNA interference (RNAi) to test the effect of down-regulation of endogenous FIP200 on S6K phosphorylation. We selected several RNAi-targeting sequences based on the human FIP200 cDNA sequence and cloned them into the RNAi vector pBS-U6 (Sui et al., 2002). One of these sequences (FIP200 #7), which showed the most significant down-regulation of FIP200 expression in preliminary studies, was used for further experiments. As shown in Fig. 5 A, transfection of RNAi vector pBS-U6-FIP200 #7 into 293T cells significantly reduced endogenous FIP200 protein level compared with 293T cells transfected with either pBS-U6 empty vector or vector pBS-U6-ctrl, which expresses an irrelevant small interfering RNA sequence. Furthermore, it had no effect on the expression of vinculin, suggesting specificity of the RNAi vector for FIP200 knockdown. Interestingly, we found that a reduction of endogenous FIP200 levels by FIP200 RNAi decreased the phosphorylation of the transfected S6K (Fig. 5 A, compare lane 3 with 1). In contrast, transfection of pBS-U6-ctrl did not affect S6K phosphorylation (Fig. 5 A, compare lane 3 with 2), suggesting that the effect on S6K phosphorylation is due to down-regulation of FIP200, but not a nonspecific effect of the RNAi pathway itself. Similar results were also obtained in HeLa cells (not depicted). We also found that knockdown of FIP200 by FIP200 RNAi reduced phosphorylation of endogenous S6K and 4EBP-1 (Fig. 5 B). Finally, we found that transfection of 293T cells with FIP200 RNAi, but not the control RNAi, reduced the size of the cells (Fig. 5 C), which is consistent with the observation that overexpression of FIP200 in 293T cells increased their size (Fig. 3). Together, these results provide further support for the idea that FIP200 regulated cell size through its effect on the TSC1–TSC2 target S6K.

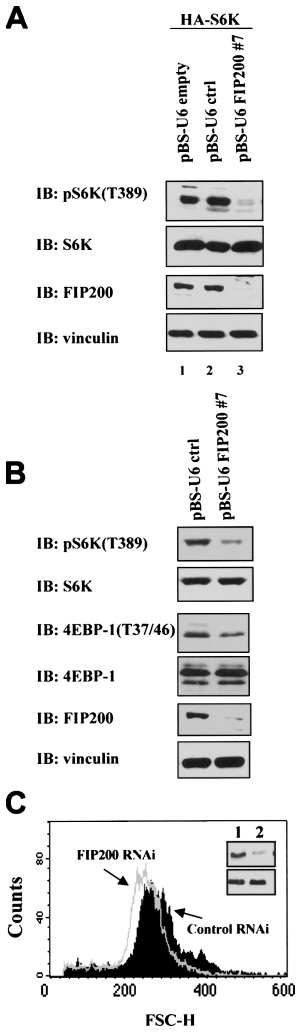

Figure 5. **Effect of down-regulation of endogenous FIP200 by RNAi on phosphorylation of S6K and cell size.** (A and B) 293T cells were transfected with HA-S6K and pBS-U6 empty vector, pBS-U6-ctrl or pBS-U6-FIP200 #7 (A), or just pBS-U6-ctrl or pBS-U6-FIP200 #7 (B). 3 d after transfection, cell lysates were analyzed by Western blotting with various antibodies, as indicated. (C) Histograms of mean FSC-H comparing 293T cells transfected with pBS-U6-FIP200 #7 (FIP200 RNAi; gray lines) with cells transfected with pBS-U6-ctrl (control RNAi). Note that a left-shift of the mean FSC-H distribution reflects cell size decrease. Inset shows the expression level of endogenous FIP200 (top) and control vinculin (bottom) in 293T cells transfected with control RNAi (lane 1) and FIP200 RNAi (lane 2).

The role of TSC1 and mTOR in the regulation of S6K and cell size by FIP200

To ensure that FIP200 regulation of S6K is through the TSC1–TSC2 complex, but not other potential mechanisms (e.g., its inhibition of FAK [Abbi et al., 2002]), we evaluated the role of TSC1 down-regulation on the decreased S6K phosphorylation on down-regulation of endogenous FIP200. TSC1 RNAi vector pBS-U6-TSC1 #3 was generated and shown to significantly decrease endogenous TSC1 protein level in 293T cells. 293T cells were then transfected with the FIP200 and TSC1 RNAi vectors, either individually or in combination, and S6K phosphorylation was then tested. As shown in Fig. 6 A, cotransfection of pBS-U6-TSC1 #3 reversed the decrease in S6K phosphorylation induced by FIP200 RNAi vector pBS-U6-FIP200 #7 (compare lane 4 and lanes 1 and 2). As expected, down-regulation of TSC1 alone also increased S6K phosphorylation (Fig. 6 A, compare lanes 1 and 3). Western blotting of the parallel samples showed that transfection of pBS-U6-TSC1 #3 decreased TSC1 expression, but had no effect on the expression of FIP200. Likewise, transfection of pBS-U6-FIP200 #7 only reduced expression of FIP200, but had no effect on TSC1 expression. Neither vector affected expression levels of vinculin

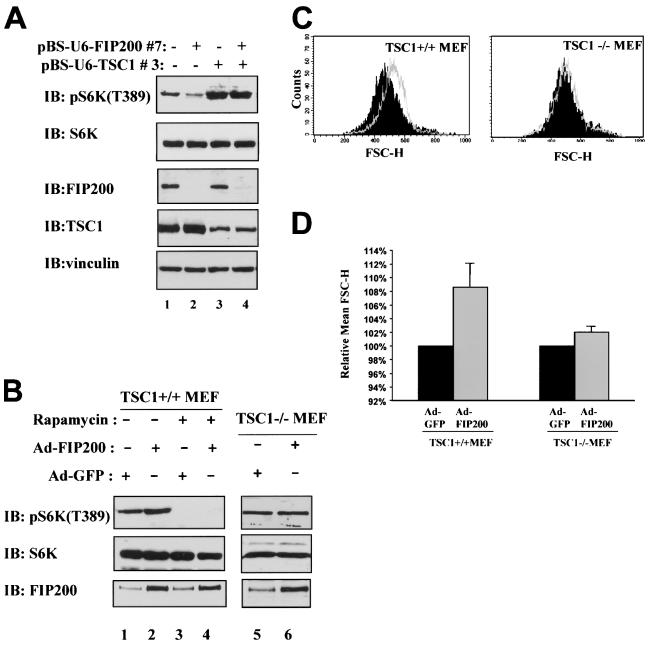

Figure 6. **FIP200 regulation of S6K phosphorylation and cell size requires TSC1 and mTOR activity.** (A) 293T cells were transfected with pBS-U6-FIP200 #7 and pBS-U6-TSC1 #3, individually or in combination, as indicated. 3 d after transfection, cell lysates were prepared and analyzed by Western blotting with various antibodies, as indicated. (B–D) TSC1−/− MEFs and control TSC1+/+ MEFs were infected with recombinant adenoviruses encoding FIP200 (Ad-FIP200) or GFP (Ad-GFP, as control), as indicated. Some samples (B, lanes 3 and 4) were treated with the mTOR inhibitor rapamycin (25 nM for 1 h). (B) Cell lysates were then analyzed by Western blotting with anti-pS6K(T389), anti-S6K, or anti-FIP200. (C) Histograms of mean FSC-H comparing cells infected with Ad-FIP200 (gray lines) to cells infected with control Ad-GFP. (D) Relative mean FSC-H + SD for three independent experiments (results are normalized to cells infected with Ad-GFP).

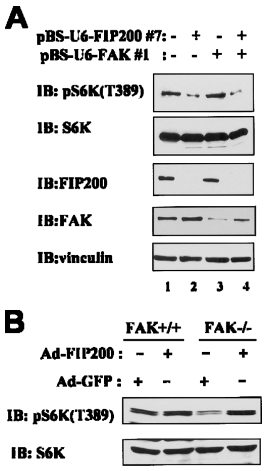

Figure 7. **Stimulation of S6K phosphorylation by FIP200 is independent of FAK.** (A) 293T cells were transfected with pBS-U6-FIP200 #7 and pBS-U6-FAK #1, individually or in combination, as indicated. 3 d after transfection, cell lysates were prepared and analyzed by Western blotting with various antibodies, as indicated. (B) FAK−/− and control FAK+/+ cells were infected with recombinant adenoviruses encoding FIP200 (Ad-FIP200) or GFP (Ad-GFP, as control), as indicated. Cell lysates were then analyzed by Western blotting with anti-pS6K(T389) or anti-S6K.

or S6K. These results demonstrate the specificity of the RNAi vectors used in the experiments.

To complement the RNAi approach, we also examined the effect of FIP200 on TSC1−/− MEFs. Fig. 6 B shows that overexpression of FIP200 increased endogenous S6K phosphorylation in TSC1+/+ MEFs, but not TSC1−/− MEFs (compare lanes 1 and 2 with lanes 5 and 6). Furthermore, we found that treatment of cells with the mTOR inhibitor rapamycin abolished stimulation of S6K phosphorylation by FIP200 (Fig. 6 B, lanes 3 and 4). Consistent with these results, we observed that overexpression of FIP200 in TSC1+/+ MEFs, but not TSC1−/− MEFs, increased cell size (Fig. 6, C and D). Together, these studies suggest that FIP200 interaction with the TSC1–TSC2 complex inhibits its function in the negative regulation of S6K activation through mTOR, which is responsible for the regulation of cell size control by FIP200.

Similar studies were performed to test a potential role of FAK in FIP200 regulation of S6K phosphorylation because previous studies showed that FIP200 could inhibit FAK, which may play a role in the activation of S6K (Malik and Parsons, 1996). Interestingly, we found that down-regulation of FAK by the RNAi vector pBS-U6-FAK #1 did not affect the reduction of S6K phosphorylation induced by pBS-U6-FIP200 #7, although it clearly down-regulated expression of FAK in these cells (Fig. 7 A). The specificity of the vectors was also demonstrated by analysis of parallel samples with anti-FIP200 and anti-vinculin. Consistent with the RNAi results, we also found that overexpression of FIP200 increased S6K phosphorylation in both FAK+/+ and FAK−/− cells (Fig. 7 B). Together, these results suggest that FIP200 regulation of S6K phosphorylation is through its inhibition of the TSC1–TSC2 complex but not FAK.

Regulation of TSC1–TSC2 complex formation by FIP200

Previous studies suggested that TSC1–TSC2 complex formation is critical for its function (Plank et al., 1998; van Slegtenhorst et al., 1998; Kwiatkowski, 2003). Therefore, we investigated whether FIP200 could affect TSC1–TSC2 complex formation to understand the mechanisms by which FIP200 regulates TSC1–TSC2 activity as shown in the aforementioned studies. 293T cells were transfected with pKH3-FIP200 or pKH3 vector as a control. TSC2 was then precipitated by anti-TSC2 antibody and the coprecipitated TSC1 was analyzed by Western blotting with anti-TSC1 antibody. As shown in Fig. 8 A, overexpression of FIP200, but not the control pKH3 vector, reduced association between TSC1 and TSC2 in these cells. Similar experiments showed that overexpression of the FIP200 N1-859 segment can also decrease TSC1–TSC2 interaction, whereas overexpression of the N1-638 segment did not (Fig. 8 B). These results raised the possibility that FIP200 may reduce the formation of the TSC1–TSC2 complex to negatively regulate its function. Surprisingly, however, knockdown of endogenous FIP200 by RNAi did not affect TSC1–TSC2 complex formation (or expression levels of TSC1 and TSC2; Fig. 8 C). These results suggested that FIP200 may inhibit TSC1–TSC2 complex function through mechanisms other than disruption of the complex formation, although we cannot exclude the possi-

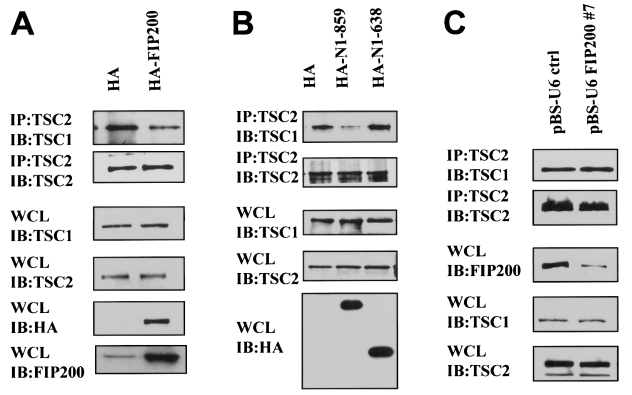

Figure 8. **Regulation of the TSC1–TSC2 complex formation by FIP200.** 293T cells were transfected with HA empty vector or HA-FIP200 (A), HA-N1-859 or HA-N1-638 (B), or pBS-U6-ctrl or pBS-U6-FIP200 #7 (C). Cell lysates were then immunoprecipitated by anti-TSC2 followed by Western blotting with anti-TSC1 to detected associated TSC1 or anti-TSC2 to verify similar amount in each samples. Cell lysates were also analyzed by Western blotting with the various antibodies indicated.

bility that it could also function to reduce the complex formation under some conditions.

Potential role of FIP200 in the regulation of the TSC-S6K pathway by nutrient level

Recent studies show that a variety of extracellular and intracellular signals such as growth factors, energy level, nutrient level, and hypoxia could regulate S6K phosphorylation through the TSC1–TSC2 complex (Gao et al., 2002; Inoki et al., 2003b; H. Zhang et al., 2003; Brugarolas et al., 2004). To examine a potential role of FIP200 in these signaling pathways, we derived FIP200−/− MEFs from FIP200 knockout mouse embryos (see Materials and methods). Fig. 9 A shows the absence of FIP200 protein expression, but similar expression levels of TSC1, TSC2, and vinculin, in the FIP200−/− MEFs compared with FIP200+/+ MEFs. We then examined the stimulation of S6K phosphorylation by various signals in FIP200−/− MEFs using FIP200+/+ MEFs as controls. We found that S6K phosphorylation was induced similarly in these two cells by serum (Fig. 9 B) and energy (Fig. 9 D) stimulations. Interestingly, FIP200−/− MEFs exhibited partial resistance to nutrient stimulation-induced S6K phosphorylation compared with the FIP200+/+ MEF controls (Fig. 9 C). Consistent with this, reduced S6 phosphorylation was also observed in FIP200−/− MEFs upon nutrient stimulation compared with FIP200+/+ MEFs. To further validate these results using FIP200−/− MEFs, we also examined stimulation of S6K phosphorylation by serum and nutrients upon FIP200 knockdown by RNAi in 293T cells. Consistent with results from FIP200−/− MEFs, FIP200 knockdown had little effect on S6K phosphorylation induced by serum (Fig. 9 E), but significantly blocked nutrient-induced S6K phosphorylation (Fig. 9 F). These results suggest that FIP200 may function in the nutrient input to the TSC1–TSC2 complex rather than being a general component of the TSC1–TSC2 to S6K pathway.

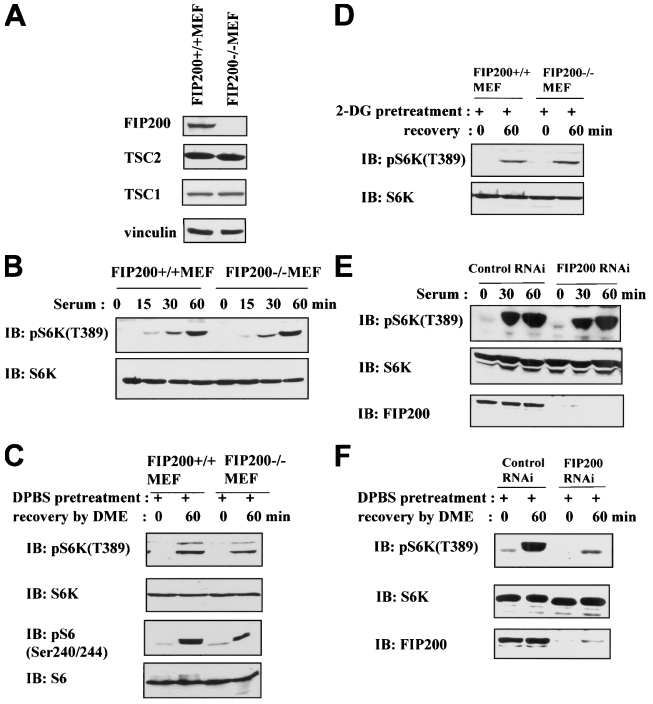

Figure 9. **Role of FIP200 in nutrient stimulation-induced activation of S6K.** (A) Cell lysates from FIP200−/−MEFs and control FIP200+/+MEFs were analyzed by Western blotting with anti-FIP200, anti-TSC2, anti-TSC1, or anti-vinculin. (B) FIP200 +/+ and FIP200−/− MEFs were serum starved overnight. They were then left untreated or treated with fresh DME + 10% FBS for the different periods of time indicated. Cell lysates were then analyzed by Western blotting with anti-pS6K(T389) and anti-S6K, respectively. (C and D) FIP200 +/+ and FIP200−/− MEFs were pretreated with DPBS + 10% FBS (C) or 50 mM 2-DG in DME + 10% FBS (D) for 60 min. They were then left untreated or retreated with fresh DME + 10% FBS for 60 min. Cell lysates were then analyzed by Western blotting with anti-pS6K(T389) and anti-S6K, respectively (C and D) as well as anti-pS6(S240/244) and anti-S6 (C). (E and F) 293T cells transfected with pBS-U6-ctrl (control RNAi) or pBS-U6-FIP200 #7 (FIP200 RNAi) were serum starved overnight (at 2 d after transfection; E) or pretreated with DPBS + 10% FBS for 60 min (at 3 d after transfection; F). They were then left untreated or treated with fresh DME + 10% FBS for the different periods of time indicated. Cell lysates were then analyzed by Western blotting with anti-pS6K(T389), anti-S6K, or anti-FIP200.

Discussion

Both cell proliferation and cell size control are fundamental biological processes that must be carefully orchestrated, and dysregulation of either can lead to diseases such as cancer. In contrast to our understanding of the mechanisms that control cell proliferation, less is known about the mechanisms that control cell size and, particularly, the mechanisms by which cell proliferation and cell size are coordinately regulated. Recently, we identified a novel protein named FIP200, which plays an important role in the regulation of cell cycle progression (Abbi et al., 2002). In this study, we showed that FIP200 can also regulate cell size through interaction with the TSC1–TSC2 complex and activation of S6K. These results identify FIP200 as a regulator that plays roles in both cell proliferation and cell size control.

Most other proteins known to play roles in both cell proliferation and cell size usually regulate these two cellular processes in a similar manner. For example, PTEN can inhibit cell

proliferation and negatively regulate cell size (Groszer et al., 2001), whereas Myc can promote cell proliferation and increase cell size (Iritani and Eisenman, 1999). In contrast, our studies indicated that FIP200 regulates cell proliferation and cell size in a differential manner, which inhibits cell proliferation but increases cell size. Interestingly, recent studies also suggested the critical cell cycle regulator pRB also plays a role in cell size control, but in a differential manner as its role in cell cycle regulation. It was shown that Rb triple knockout MEFs (triple knockout MEFs lacking all three Rb family proteins pRb, p107, and p130) have increased cell proliferation, but a significantly reduced cell size compared with control MEFs (Sage et al., 2000). It is interesting to note that FIP200 has been reported to up-regulate RB1 expression in recent studies by Chano and co-workers (Chano et al., 2002a; Kontani et al., 2003), although it remains to be determined whether the pRB pathway is involved in the regulation of cell size by FIP200. Nevertheless, data presented in this study strongly suggest that FIP200 regulates cell size through its interaction with the TSC1–TSC2 complex.

Our previous study showed that FIP200 plays an important role in cell proliferation; however, little is known about the targets and molecular mechanisms by which FIP200 regulates cell proliferation. Several studies also suggest the important role of the TSC1–TSC2 complex in cell cycle control. Overexpression of TSC1 or TSC2 can inhibit cell cycle progression (Soucek et al., 1998, 2001; Miloloza et al., 2000; Hengstschlager and Rosner, 2003). TSC2 has been shown to interact with several cell cycle regulators such as cdk1, cyclin A, and cyclin B (Catania et al., 2001). Furthermore, TSC2 was shown to stabilize p27 and negatively regulate cdk2 function (Soucek et al., 1998). However, recent studies using TSC1 and TSC2 null MEFs showed decreased proliferation (instead of increased proliferation as would be predicted from the overexpression studies) compared with control MEFs (Y. Zhang et al., 2003). Furthermore, both TSC1 and TSC2 have been shown to be required for serum stimulation of Akt activation, which plays critical roles in cell proliferation and cell survival (Kwiatkowski et al., 2002; Y. Zhang et al., 2003). Therefore, the function of TSC in the regulation of cell proliferation is complicated. We initially hypothesized that the interaction between FIP200 and the TSC1–TSC2 complex would play a role in FIP200-mediated cell cycle progression. However, we found that FIP200 can inhibit cell cycle progression in TSC1−/− MEFs as well as control MEFs. In addition, the FIP200 N1-638 segment does not interact with the TSC1–TSC2 complex but still inhibits cell cycle progression. Together, these data suggest that interaction between FIP200 and the TSC1–TSC2 complex is not involved in FIP200-mediated cell cycle progression.

Our results demonstrated that FIP200 functions to positively regulate cell size and S6K phosphorylation. Although we cannot exclude completely the possible role of other as yet unidentified proteins that interact with FIP200, current evidence suggests that these effects are through FIP200 interaction with the TSC1–TSC2 complex. We found that association of FIP200 or its segments N1-859 and N1-638 with the TSC1–TSC2 complex correlated with their ability to increase cell size, up-regulate S6K phosphorylation, and decrease TSC1–TSC complex formation. Conversely, knockdown of endogenous FIP200 by RNAi reduced S6K phosphorylation and cell size. We also observed that FIP200 RNAi has no effect on S6K phosphorylation in TSC1 knockdown cells but can decrease S6K phosphorylation in control cells. Consistent with this, FIP200 failed to stimulate S6K phosphorylation and increase cell size in TSC1-null MEFs in contrast to control MEFs and that the stimulatory effect in control MEFs was abolished by rapamycin. These results suggested that the TSC1–TSC2 complex and its downstream target mTOR are required for FIP200 regulation of S6K phosphorylation. Using both RNAi approach and FAK−/− cells, we showed that FIP200 inhibition of FAK is not involved in the regulation of S6K phosphorylation by FIP200.

Recent studies have established the TSC1–TSC2 complex as a key regulator of cell size control, and rapid progress has been made in delineating the downstream biochemical pathways by which TSC regulates cell size as well as their roles in the regulation of other cellular functions (Hengstschlager et al., 2001; Inoki et al., 2003b; Kwiatkowski, 2003; Shamji et al., 2003). In contrast, relatively little is known about the molecular mechanisms by which TSC is regulated by upstream regulators. Several proteins have been shown to interact with TSC2 and thus regulate the TSC1–TSC2 complex function. Protein kinases AKT and AMPK have been identified to phosphorylate TSC2 and negatively and positively regulate TSC1–TSC2 complex function, respectively (Inoki et al., 2002, 2003b). 14-3-3 was shown to interact with and negatively regulate TSC2 without affecting TSC1–TSC2 interaction (Li et al., 2002; Shumway et al., 2003). ERM family proteins and neurofilament-light chain were shown to interact with TSC1, but it is not clear whether these interactions regulate TSC1–TSC2 complex function (Lamb et al., 2000; Haddad et al., 2002). Here, we identified a novel interaction between FIP200 and TSC1 and provided evidence suggesting that this interaction could negatively regulate TSC1–TSC2 complex function to increase S6K phosphorylation and cell size. This is the first paper suggesting a regulatory mechanism through protein interaction with TSC1 of the complex.

Our results suggested that FIP200 is important for nutrient stimulation-induced, but not energy- or serum-induced, S6K activation (Fig. 9). Nutrient-induced S6K phosphorylation was lower in FIP200−/− MEFs compared with FIP200+/+ MEFs as well as in 293T cells treated with FIP200 RNAi compared with cells treated with control RNAi (Fig. 9, C and F). However, we noted that the decrease was moderate in the FIP200−/− MEFs, whereas it was greater in the short-term RNAi knockdown experiments. This could be due to differences in the cells used in these two different sets of experiments. Alternatively, FIP200−/− MEFs may have adapted to the FIP200 null condition during the culture (thus becoming less dependent on FIP200 for nutrient-induced S6K phosphorylation). However, we tested the expression levels of TSC1 and TSC2 in these cells and found that their expression levels are similar to those in FIP200+/+ MEFs, suggesting that there is no compensatory changes in either TSC1 or TSC2 expression

in the FIP200−/−MEFs. Future studies will be necessary to determine whether expression of other genes is altered, which could partially compensate for the loss of FIP200 in nutrient-stimulated S6K phosphorylation. Nevertheless, these results suggest that FIP200 functions in the nutrient input to the TSC1–TSC2 complex rather than being a general component of the TSC1–TSC2 signaling pathway.

The molecular mechanisms by which FIP200 interaction with TSC1 inhibits TSC1–TSC2 functions are not clear at present. We found that overexpression of FIP200 reduced TSC1–TSC2 complex formation (Fig. 8, A and B), raising the possibility that FIP200 could inhibit TSC1–TSC2 function by disrupting the complex formation. However, several considerations would argue against such a possible mechanism. First, knockdown of endogenous FIP200 by RNAi did not significantly promote endogenous TSC1–TSC2 complex formation (Fig. 8 C). Second, although our binding studies suggested that TSC1 coiled-coil region mediates its interaction with TSC2 (unpublished data), the relevant functional segment of FIP200 (N1-859) does not contain its COOH-terminal coiled-coil region. Furthermore, the FIP200 binding region in TSC1 resides in residues 403–787, which overlaps little with the putative coiled-coil region of TSC1 (residues 719–998; also see Fig. 1 A). Thus, it is unlikely that FIP200 could disrupt TSC1–TSC2 interaction simply by its coiled-coil domain binding to the coiled-coil region of TSC1 and displace TSC2 from its association with TSC1. Lastly, we observed that FIP200 could coimmunoprecipitate both endogenous (Fig. 1 E) and transfected (Fig. 2 A) TSC2, which would not be possible if FIP200 functioned to disrupt the complex by competing with TSC2 for TSC1 binding. Although we cannot completely exclude the possibility that FIP200 could function to reduce the TSC1–TSC2 complex formation under some conditions, the aforementioned consideration would suggest that FIP200 may inhibit TSC1–TSC2 complex function through mechanisms other than disruption of the complex formation. It is possible that FIP200 binding to TSC1 may also inhibit TSC1–TSC2 function by inducing conformational change in TSC2 (indirectly through TSC1) to inhibit its GAP activity toward Rheb. Future studies will be necessary to investigate such a possible mechanism.

In summary, our studies identified FIP200 as a novel interacting protein with TSC1 and suggested that FIP200 could negatively regulate TSC function. These results indicate that, in addition to its function in cell cycle progression, FIP200 also plays a role in cell size control. Furthermore, they provide new insight into the molecular mechanism of TSC regulation. These studies raise interesting implications regarding the molecular mechanisms by which cell proliferation and cell size are coordinately regulated and, potentially, how dysregulation of cell cycle progression and cell size control lead to diseases such as cancer.

Materials and methods

Antibodies and reagents

The rabbit antiserum against FIP200 has been described previously (Abbi et al., 2002). The polyclonal and monoclonal TSC1 antibodies were gifts of V. Ramesh (Massachusetts General Hospital, Boston, MA). Affinity-purified antibody against GST was prepared from anti-GST serum using GST immobilized on glutathione-Sepharose as an affinity matrix. The mouse monoclonal α-vinculin antibody was obtained from Upstate Biotechnology. The rabbit polyclonal α-HA (Y11) antibody, the mouse monoclonal α-c-Myc-tag (9E10) antibody, rabbit polyclonal TSC2 antibody, rabbit polyclonal α-FAK (C20) antibody, and rabbit polyclonal S6K antibody were obtained from Santa Cruz Biotechnology, Inc. S6, Ser240/244 phospho-S6, Thr389 phospho-S6K, Thr37/46 phospho-4E-BP1, Ser65 phospho-4E-BP-1, and 4E-BP-1 antibodies were purchased from Cell Signaling Inc. Rapamycin was obtained from Calbiochem. DPBS was purchased from Invitrogen. 2-Deoxy-D-Glucose (2-DG) was obtained from Sigma-Aldrich.

Yeast two-hybrid assays

The vector pLexA-FIP200 N1-859 was used to screen a human heart MATCHMAKER LexA cDNA library (>10^6 independent clones; gift from C. Wu, University of Pittsburgh, Pittsburgh, PA). The yeast two-hybrid screen was performed essentially as described previously (Tu et al., 1999).

Cell culture

The FIP200$^{-/-}$ and control MEFs were isolated from E12.5 embryos. The early passage (P1–P3) MEFs were used for studies here. The TSC1$^{-/-}$ and control MEFs were a gift of D. Kwiatkowski (Brigham and Women's Hospital, Boston, MA) and were maintained in DME supplemented with 10% FBS as described previously (Kwiatkowski et al., 2002). The FAK$^{-/-}$ fibroblasts derived from the FAK-null mouse embryos were a gift of D. Ilic (University of California, San Francisco, San Francisco, CA) and were maintained in DME supplemented with 10% FBS. 293T cells were cultured in DME supplemented with 10% FBS. NIH3T3 cells were maintained in DME supplemented with 10% CS.

Plasmid DNA construction

The vectors used in the yeast two-hybrid screen, pLexA, pLexA-Lamin C, and pB42AD, have been described previously (Tu et al., 1999). pKH3-FIP200 was used as a template to generate pLexA-FIP200 N1-859: the PCR fragment amplified by primers 5′-gaattcatgaagttatatgtatttctgg-3′ (forward) and 5′-ctcgagtagtgttatttccagagaaca-3′ (reverse) was first inserted into pGEMT (BD Biosciences), then digested with XhoI and EcoRI, and the fragment was then inserted into pLexA (BD Biosciences) digested with the same enzymes to generate pLexA-FIP200 N1-859.

The mammalian cell expression vectors pKH3, pKH3-FIP200, and pKH3- FIP200 N1-638 have been described previously (Abbi et al., 2002). pKH3-FIP200 was used as a template to produce pKH3-FIP200 N1-859: the PCR product with primers 5′-cgcggatccatgaagttatatgtatttctgg-3′ (forward) and 5′-cccatcgattcatagtcttatttccagagaacattt-3′ (reverse) was digested with BamHI and ClaI. The fragment was then ligated to a linearized pKH3 vector digested with the same enzymes. The same PCR product was digested with BamHI and ClaI and then inserted into linearized pMAL at the corresponding sites to generate pMAL-FIP200-N859, which is then used to express MBP-N1-859 fusion protein from bacteria.

The expression vectors encoding HA-S6K, Flag-4EBP1, HA-TSC2, GST-TSC2, Myc-TSC1, and Myc-TSC1 1–402 aa have been described previously (Inoki et al., 2002, 2003a,b). Myc-TSC1 was used as template to generate the following construct: the TSC1 789–1165 aa fragment was amplified by primers 5′-cgcggatccgaattcgacaaccagagccaggaa-3′ (forward) and 5′-cccatcgatttagctgttttcatgatgagtctc-3′ (reverse), digested with BamHI and ClaI, and then inserted into linearized myc-tagged vector pHAN digested with BamHI and ClaI, resulting in Myc-TSC1 789–1165 aa. The TSC1 403–787 aa fragment was amplified by primers 5′-cgcggatccgatgactacgtgcacatttca-3′ (forward) and 5′-cccatcgatctggctctggttgtagaatcc-3′ (reverse), digested with BamHI and ClaI, and then inserted into linearized myc-tagged vector pHAN digested with the same enzymes, resulting in Myc-TSC1 403–787 aa. The same PCR product was digested with BamHI and ClaI and then inserted into linearized pGEX2T at the corresponding sites to generate pGEX2T-TSC1 403–787 aa, which is then used to express the GST-TSC1 403–787 aa fusion protein from bacteria. The enzymes used in cloning were all obtained from New England Biolabs, Inc. Nucleotide sequences of all constructs were confirmed by DNA sequencing.

Immunoprecipitation and Western blotting

Preparation of whole cell lysates, immunoprecipitation, and Western blotting were performed as previously described (Abbi et al., 2002).

Preparation of GST, MBP fusion proteins, and in vitro binding assays

GST fusion proteins were produced and purified as described previously (Abbi et al., 2002). MBP fusion proteins were purified according to the

manufacturer's instructions (New England Biolabs, Inc.). MBP and MBP-N1-859 fusion proteins (10 μg) were immobilized on amylose resin and then incubated at 4°C with 2 μg GST-TSC1 403–787 in binding buffer (20 mM Tris, pH 8.0, 137 mM NaCl, 1 mM $MgCl_2$, and 1% Triton X-100) overnight at 4°C with rotation. The samples were then washed five times with binding buffer, boiled in SDS buffer, resolved by SDS-PAGE, and analyzed by Western blotting anti-GST antibody.

RNAi constructs and transfection

The RNAi vector pBS-U6 is a gift from Y. Shi (Harvard Medical School, Boston, MA) and has been described previously (Sui et al., 2002). Construction of RNAi vector was achieved in two separate steps: a 22-nt oligo (oligo 1) was first inserted into the pBS-U6 vector digested with ApaI (blunted) and HindIII. The inverted motif that contains the 6-nt spacer and 5 Ts (oligo 2) was then subcloned into the HindIII and EcoRI sites of the intermediate plasmid to generate pBS-U6-FIP200. For pBS-U6-FIP200 #7, the sequence of oligo1 is 5′-GGAGATTTGGTACTCATCATCA-3′ (forward) and 5′-AGCTTGATGATGAGTACCAAATCTCC-3′ (reverse); the sequence of oligo2 is 5′-AGCTTGATGATGAGTACCAAATCTCCCTTTTTG-3′ (forward) and 5′-AATTCAAAAAGGGAGATTTGGTACTCATCATCA-3′ (reverse). For pBS-U6-TSC1 #3, the sequence of oligo1 is 5′-GGGAGGTCAACGAGCTCTATTA (forward) and 5′-AGCTTAATAGAGCTCGTTGACCTCCC-3′ (reverse); the sequence of oligo2 is 5′-AGCTTAATAGAGCTCGTTGACCTCCCCTTTTTG-3′ (forward) and 5′-AATTCAAAAAGGGGAGGTCAACGAGCTCTATTA (reverse). For pBS-U6-FAK #1, the sequence of oligo1 is 5′-GGCCAGTATTATCAGGCATGGA-3′ (forward) and 5′-AGCTTCCATGCCTGATAATACTGGCC-3′ (reverse); the sequence of oligo2 is 5′-AGCTTCCATGCCTGATAATACTGGCCCTTTTTG-3′ (forward) and 5′-AATTCAAAAAGGGCCAGTATTATCAGGCATGGA-3′ (reverse). The RNAi targeting sequences were all analyzed by BLAST search to ensure that they did not have significant sequence homology with other genes.

For RNAi knockdown experiments, 293T cells grown in 6-well plates were transfected with 1 μg RNAi vectors and 50 ng HA-S6K constructs using Lipofectamine reagent (Invitrogen) in accordance with the manufacturer's instructions. For double knockdown experiments, 293T cells were transfected with two RNAi vectors, each 500 ng, and 50 ng HA-S6K constructs. To detect endogenous S6K phosphorylation, cells grown in 6-well plates were transfected with 1 μg RNAi vectors without HA-S6K construct. After 3 d, growing cells were either directly lysed for Western blotting or used for growth factor and nutrient stimulation experiments as mentioned in the corresponding legends.

Cell size assay

To determine cell size and DNA content, FACS analysis with Cell Quest software was performed as previously described (Inoki et al., 2003b).

We are grateful to Dr. Vijaya Ramesh for anti-TSC1 antibody, Dr. Cary Wu for the yeast two-hybrid vectors and a human heart cDNA library, Dr. Yang Shi for the RNAi vector pBS-U6, Dr. David Kwiatkowski for TSC1−/− cells, and Dr. Dusko Ilic for FAK−/− cells. We thank Xu Peng, Dan Rhoads, and Huijun Wei for their critical reading of the manuscript and helpful comments.

This research was supported by National Institutes of Health grant GM52890 to J.-L. Guan.

Submitted: 17 November 2004
Accepted: 30 June 2005

References

Abbi, S., H. Ueda, C. Zheng, L.A. Cooper, J. Zhao, R. Christopher, and J.L. Guan. 2002. Regulation of focal adhesion kinase by a novel protein inhibitor FIP200. *Mol. Biol. Cell.* 13:3178–3191.

Brugarolas, J., K. Lei, R.L. Hurley, B.D. Manning, J.H. Reiling, E. Hafen, L.A. Witters, L.W. Ellisen, and W.G. Kaelin Jr. 2004. Regulation of mTOR function in response to hypoxia by REDD1 and the TSC1/TSC2 tumor suppressor complex. *Genes Dev.* 18:2893–2904.

Catania, M.G., P.S. Mischel, and H.V. Vinters. 2001. Hamartin and tuberin interaction with the G2/M cyclin-dependent kinase CDK1 and its regulatory cyclins A and B. *J. Neuropathol. Exp. Neurol.* 60:711–723.

Chano, T., S. Ikegawa, K. Kontani, H. Okabe, N. Baldini, and Y. Saeki. 2002a. Identification of RB1CC1, a novel human gene that can induce RB1 in various human cells. *Oncogene.* 21:1295–1298.

Chano, T., S. Ikegawa, F. Saito-Ohara, J. Inazawa, A. Mabuchi, Y. Saeki, and H. Okabe. 2002b. Isolation, characterization and mapping of the mouse and human RB1CC1 genes. *Gene.* 291:29–34.

Chano, T., K. Kontani, K. Teramoto, H. Okabe, and S. Ikegawa. 2002c. Truncating mutations of RB1CC1 in human breast cancer. *Nat. Genet.* 31:285–288.

Chano, T., Y. Saeki, M. Serra, K. Matsumoto, and H. Okabe. 2002d. Preferential expression of RB1-inducible coiled-coil 1 in terminal differentiated musculoskeletal cells. *Am. J. Pathol.* 161:359–364.

Dahiya, R., G. Perinchery, G. Deng, and C. Lee. 1998. Multiple sites of loss of heterozygosity on chromosome 8 in human breast cancer has differential correlation with clinical parameters. *Int. J. Oncol.* 12:811–816.

Gao, X., Y. Zhang, P. Arrazola, O. Hino, T. Kobayashi, R.S. Yeung, B. Ru, and D. Pan. 2002. Tsc tumour suppressor proteins antagonize amino-acid-TOR signalling. *Nat. Cell Biol.* 4:699–704.

Garami, A., F.J. Zwartkruis, T. Nobukuni, M. Joaquin, M. Roccio, H. Stocker, S.C. Kozma, E. Hafen, J.L. Bos, and G. Thomas. 2003. Insulin activation of Rheb, a mediator of mTOR/S6K/4E-BP signaling, is inhibited by TSC1 and 2. *Mol. Cell.* 11:1457–1466.

Goncharova, E.A., D.A. Goncharov, A. Eszterhas, D.S. Hunter, M.K. Glassberg, R.S. Yeung, C.L. Walker, D. Noonan, D.J. Kwiatkowski, M.M. Chou, et al. 2002. Tuberin regulates p70 S6 kinase activation and ribosomal protein S6 phosphorylation. A role for the TSC2 tumor suppressor gene in pulmonary lymphangioleiomyomatosis (LAM). *J. Biol. Chem.* 277:30958–30967.

Groszer, M., R. Erickson, D.D. Scripture-Adams, R. Lesche, A. Trumpp, J.A. Zack, H.I. Kornblum, X. Liu, and H. Wu. 2001. Negative regulation of neural stem/progenitor cell proliferation by the Pten tumor suppressor gene in vivo. *Science.* 294:2186–2189.

Haddad, L.A., N. Smith, M. Bowser, Y. Niida, V. Murthy, C. Gonzalez-Agosti, and V. Ramesh. 2002. The TSC1 tumor suppressor hamartin interacts with neurofilament-L and possibly functions as a novel integrator of the neuronal cytoskeleton. *J. Biol. Chem.* 277:44180–44186.

Hengstschlager, M., and M. Rosner. 2003. The cell cycle and tuberous sclerosis. *Prog. Cell Cycle Res.* 5:43–48.

Hengstschlager, M., D.M. Rodman, A. Miloloza, E. Hengstschlager-Ottnad, M. Rosner, and M. Kubista. 2001. Tuberous sclerosis gene products in proliferation control. *Mutat. Res.* 488:233–239.

Inoki, K., Y. Li, T. Zhu, J. Wu, and K.L. Guan. 2002. TSC2 is phosphorylated and inhibited by Akt and suppresses mTOR signalling. *Nat. Cell Biol.* 4:648–657.

Inoki, K., Y. Li, T. Xu, and K.L. Guan. 2003a. Rheb GTPase is a direct target of TSC2 GAP activity and regulates mTOR signaling. *Genes Dev.* 17: 1829–1834.

Inoki, K., T. Zhu, and K.L. Guan. 2003b. TSC2 mediates cellular energy response to control cell growth and survival. *Cell.* 115:577–590.

Iritani, B.M., and R.N. Eisenman. 1999. c-Myc enhances protein synthesis and cell size during B lymphocyte development. *Proc. Natl. Acad. Sci. USA.* 96:13180–13185.

Kontani, K., T. Chano, Y. Ozaki, N. Tezuka, S. Sawai, S. Fujino, Y. Saeki, and H. Okabe. 2003. RB1CC1 suppresses cell cycle progression through RB1 expression in human neoplastic cells. *Int. J. Mol. Med.* 12:767–769.

Kwiatkowski, D.J. 2003. Tuberous sclerosis: from tubers to mTOR. *Ann. Hum. Genet.* 67:87–96.

Kwiatkowski, D.J., H. Zhang, J.L. Bandura, K.M. Heiberger, M. Glogauer, N. el-Hashemite, and H. Onda. 2002. A mouse model of TSC1 reveals sex-dependent lethality from liver hemangiomas, and up-regulation of p70S6 kinase activity in Tsc1 null cells. *Hum. Mol. Genet.* 11:525–534.

Lamb, R.F., C. Roy, T.J. Diefenbach, H.V. Vinters, M.W. Johnson, D.G. Jay, and A. Hall. 2000. The TSC1 tumour suppressor hamartin regulates cell adhesion through ERM proteins and the GTPase Rho. *Nat. Cell Biol.* 2:281–287.

Li, Y., K. Inoki, R. Yeung, and K.L. Guan. 2002. Regulation of TSC2 by 14-3-3 binding. *J. Biol. Chem.* 277:44593–44596.

Malik, R.K., and J.T. Parsons. 1996. Integrin-dependent activation of the p70 ribosomal S6 kinase signaling pathway. *J. Biol. Chem.* 271:29785–29791.

Manning, B.D., A.R. Tee, M.N. Logsdon, J. Blenis, and L.C. Cantley. 2002. Identification of the tuberous sclerosis complex-2 tumor suppressor gene product tuberin as a target of the phosphoinositide 3-kinase/akt pathway. *Mol. Cell.* 10:151–162.

Miloloza, A., M. Rosner, M. Nellist, D. Halley, G. Bernaschek, and M. Hengstschlager. 2000. The TSC1 gene product, hamartin, negatively regulates cell proliferation. *Hum. Mol. Genet.* 9:1721–1727.

Plank, T.L., R.S. Yeung, and E.P. Henske. 1998. Hamartin, the product of the tuberous sclerosis 1 (TSC1) gene, interacts with tuberin and appears to be localized to cytoplasmic vesicles. *Cancer Res.* 58:4766–4770.

Potter, C.J., H. Huang, and T. Xu. 2001. *Drosophila* Tsc1 functions with Tsc2 to antagonize insulin signaling in regulating cell growth, cell proliferation, and organ size. *Cell.* 105:357–368.

Sage, J., G.J. Mulligan, L.D. Attardi, A. Miller, S. Chen, B. Williams, E. Theodorou, and T. Jacks. 2000. Targeted disruption of the three Rb-related genes leads to loss of G(1) control and immortalization. *Genes Dev.* 14:3037–3050.

Saucedo, L.J., X. Gao, D.A. Chiarelli, L. Li, D. Pan, and B.A. Edgar. 2003. Rheb promotes cell growth as a component of the insulin/TOR signalling network. *Nat. Cell Biol.* 5:566–571.

Shamji, A.F., P. Nghiem, and S.L. Schreiber. 2003. Integration of growth factor and nutrient signaling: implications for cancer biology. *Mol. Cell.* 12:271–280.

Shumway, S.D., Y. Li, and Y. Xiong. 2003. 14-3-3beta binds to and negatively regulates the tuberous sclerosis complex 2 (TSC2) tumor suppressor gene product, tuberin. *J. Biol. Chem.* 278:2089–2092.

Soucek, T., R.S. Yeung, and M. Hengstschlager. 1998. Inactivation of the cyclin-dependent kinase inhibitor p27 upon loss of the tuberous sclerosis complex gene-2. *Proc. Natl. Acad. Sci. USA.* 95:15653–15658.

Soucek, T., M. Rosner, A. Miloloza, M. Kubista, J.P. Cheadle, J.R. Sampson, and M. Hengstschlager. 2001. Tuberous sclerosis causing mutants of the TSC2 gene product affect proliferation and p27 expression. *Oncogene.* 20:4904–4909.

Stocker, H., T. Radimerski, B. Schindelholz, F. Wittwer, P. Belawat, P. Daram, S. Breuer, G. Thomas, and E. Hafen. 2003. Rheb is an essential regulator of S6K in controlling cell growth in *Drosophila*. *Nat. Cell Biol.* 5:559–565.

Sui, G., C. Soohoo, E.B. Affar, F. Gay, Y. Shi, W.C. Forrester, and Y. Shi. 2002. A DNA vector-based RNAi technology to suppress gene expression in mammalian cells. *Proc. Natl. Acad. Sci. USA.* 99:5515–5520.

Tapon, N., N. Ito, B.J. Dickson, J.E. Treisman, and I.K. Hariharan. 2001. The *Drosophila* tuberous sclerosis complex gene homologs restrict cell growth and cell proliferation. *Cell.* 105:345–355.

Tee, A.R., B.D. Manning, P.P. Roux, L.C. Cantley, and J. Blenis. 2003. Tuberous sclerosis complex gene products, Tuberin and Hamartin, control mTOR signaling by acting as a GTPase-activating protein complex toward Rheb. *Curr. Biol.* 13:1259–1268.

Tu, Y., F. Li, S. Goicoechea, and C. Wu. 1999. The LIM-only protein PINCH directly interacts with integrin-linked kinase and is recruited to integrin-rich sites in spreading cells. *Mol. Cell. Biol.* 19:2425–2434.

Ueda, H., S. Abbi, C. Zheng, and J.L. Guan. 2000. Suppression of Pyk2 kinase and cellular activities by FIP200. *J. Cell Biol.* 149:423–430.

van Slegtenhorst, M., M. Nellist, B. Nagelkerken, J. Cheadle, R. Snell, A. van den Ouweland, A. Reuser, J. Sampson, D. Halley, and P. van der Sluijs. 1998. Interaction between hamartin and tuberin, the TSC1 and TSC2 gene products. *Hum. Mol. Genet.* 7:1053–1057.

Zhang, H., G. Cicchetti, H. Onda, H.B. Koon, K. Asrican, N. Bajraszewski, F. Vazquez, C.L. Carpenter, and D.J. Kwiatkowski. 2003. Loss of Tsc1/Tsc2 activates mTOR and disrupts PI3K-Akt signaling through downregulation of PDGFR. *J. Clin. Invest.* 112:1223–1233.

Zhang, Y., X. Gao, L.J. Saucedo, B. Ru, B.A. Edgar, and D. Pan. 2003. Rheb is a direct target of the tuberous sclerosis tumour suppressor proteins. *Nat. Cell Biol.* 5:578–581.

Zhao, J.H., H. Reiske, and J.L. Guan. 1998. Regulation of the cell cycle by focal adhesion kinase. *J. Cell Biol.* 143:1997–2008.